DYNAMIC PROPERTIES OF AN EARTHQUAKE SOURCE

by

Paul G. Richards [I]

SYNOPSIS

Motions at and near an earthquake source are investigated theoretically and numerically. The source is modeled by a crack across which the shear stress is dropped to some constant times the normal stress: the crack nucleates from a point, and then grows steadily as an ellipse with fixed eccentricity. The solution allows rapid computation of the accelerations radiated, at all points in space and time. At about 1 km. from the fault surface, but 10 km. from the point of initial rupture, accelerations reach up to about 1/2 g (per 100 bars of stress drop) as the rupture front passes nearby.

INTRODUCTION

Earthquakes are the immediate result of some rupture process, which spreads rapidly in time over a zone in which stress has previously been slowly accumulating. Evidence on the kinematics of this rupture process is available from geological and engineering field studies, from distribution of the first motions radiated by the source, and from our understanding of large-scale tectonic motions. Such studies all indicate that the earthquake mechanism commonly involves shear failure across a planar fault surface. This paper is concerned with describing a source model which fits the observed kinematics of such ruptures; which is also dynamically satisfactory in terms of the stresses existing at the earthquake focus; and which permits the solution and computation of all source motions and radiated motions. Several sample computations are described.

[I] Assistant Professor of Geology, Lamont-Doherty Geological Observatory of Columbia University, Palisades, New York.

SPECIFICATION OF SOURCE PROPERTIES AND ELASTICITY PROBLEM

We consider a homogeneous elastic medium, and take an earthquake source to involve a plane (fault) surface, across which discontinuous displacements arise in directions parallel to the fault. Burridge and Knopoff[1] have shown that specification merely of the shear dislocation permits an explicit solution to be stated for displacement throughout the medium, but this important result does not directly help to answer the question of what dislocations are likely. Since the rupture involves shear failure, the choice of dislocation must satisfy not only a kinematic description of shearing motion across a fault, but also dynamic constraints on the components of traction across the fault surface. The physics of the faulting process determine these constraints, and we shall assume that shear stresses on the new fault surface, after a rupture front has passed by and initiated relative motion between opposite faces of the fault, are entirely frictional, being proportional to the normal stress. This physical assumption is much simpler than might be expected, since it may be shown (by inspection of symmetries in the displacement formulae of Haskell[2] for the radiation from a shear dislocation) that the normal stress stays constant throughout the rupture process. So the shear stress on the new fault surface is time independent, and linearity permits us to consider the problem in terms merely of stress drop.

The above remarks are relevant to problems even with an inhomogeneous initial stress, and unsteady rupture propagation. But the particular source to be taken up below is further simplified by dropping these two features, thereby yielding a tractable problem, though one which still is of practical relevance to our understanding of the rupture process in earthquakes.

Specifically, we assume initially a state of uniform stress $\underset{\sim}{\sigma}^{\circ}$, and at time $t = 0$ a plane shear crack nucleates at the origin. The fault surface $S(t)$ is defined in cartesian coordinates by the ellipse

$$S(t) = \{z = 0: \quad x^2/\sigma^2 + y^2/\nu^2 \leqslant t^2\} \tag{1}$$

which (see Figure 1) has axes which grow steadily at speeds σ and ν, each less than the shear wave speed, c_s. The shear stresses across plane $z = 0$ are influenced by waves emanating from the point of nucleation, but after arrival of the rupture they drop to values σ^1_{yz}, σ^1_{zx}, which are constant over $S(t)$. Because of radiation from previous growth of the crack, we do not immediately know the value (at a given point in the fault plane) the stress drops down from, at the arrival of rupture.

To describe the problem further, we let $\underset{\sim}{u}$ be displacement away from the initial (prestressed, static) position, with $\underset{\approx}{\tau}$ as the derived stress tensor (so that $\underset{\approx}{\sigma}^{\circ} + \underset{\approx}{\tau}$ is the total stress). To set up a boundary value problem, we note that constancy of normal stress across the fault plane implies

$$\tau_{zz} = 0 \quad \text{everywhere on } z = 0 \tag{2}$$

Our assumption that shear stresses on the new crack surface are purely frictional implies

$$(\tau_{zx}, \tau_{zy}) = (\sigma^{\circ}_{zz}\mu_f \cos\psi - \sigma^{\circ}_{zx}\ ,\ \sigma^{\circ}_{zz}\mu_f \sin\psi - \sigma^{\circ}_{zy}) \text{ on } S(t) \quad (3)$$

in which ψ specifies the frictional force direction, and μ_f is the coefficient of dynamic friction. The principal property here is that shear stresses are constant over S(t).

It may be expected that our problem of solving for the vector displacement will require three conditions over the total boundary surface $z = 0$. Equation (2) is one such condition, and (3) is two conditions for part of the boundary. Two more conditions for the remaining part of the boundary can also be stated. They are conditions on the shearing displacements, which Haskell's [2] formulae show to be odd functions of z, the distance from the fault. Since they are also continuous except across S(t), we conclude

$$u_x = u_y = 0, \quad \text{on } z = 0 \text{ but off } S(t). \quad (4)$$

Solving for the elastic motion, conditioned by (2), (3) and (4), thus appears to be a mixed boundary value problem. However, a greatly simplified ordinary boundary value problem can instead be set up, using the work of Burridge and Willis [3], who found the discontinuity in shearing displacements across S(t), for the present problem of an elliptical crack. Their work, together with Haskell's [2], implies that

$$(u_x, u_y) = \begin{cases} (0,0) & \text{on } z = 0^+ \text{ but off } S(t) \\ (a, b)\ (t^2 - x^2/\sigma^2 - y^2/\nu^2)^{1/2} & \text{on } z = 0^+ \text{ and } S(t). \end{cases} \quad (5)$$

Note that the displacement of the origin (point of nucleation) has components (at, bt) after rupturing, so the constant (a, b) velocities are just particle velocities for the center of the crack. Conditions (2) and (5) are now in the form which establish a boundary value problem for the elastic radiation into $z > 0$. Radiation into $z < 0$ can be determined by symmetry, or by setting up boundary values on $z = 0^-$.

Burridge and Willis [3] have shown that shear stress drops (τ_{zx}, τ_{zy}) are proportional to the source particle velocities (a, b). We now turn to a brief description of the radiation solution, for the case that $b = 0$, i.e. for relief of initial stress component σ°_{zx}.

SOLUTION METHOD

Although formal displacement solutions may be set up for many interesting problems of fracture, few representations permit calculation of the motion without major and sophisticated computation - the effort involved suppressing most attempts. Thus, knowledge of the dislocation (5) permits a surface integral [2] to be written down for the radiation.

The integrand, however, is singular, and numerical stability has not been achieved even in computations with a dislocation which does not generate a singular integrand. Burridge and Willis [3] have obtained a solution for the present problem, also involving a surface integral, but their representation appears computationally even more intractable.

The present method, outlined below and given in more detail by Richards,[4] gives acceleration and stress-rates, at all positions and times, in terms of single integrals plus algebraic expressions. The integrands are non-singular, and the solution has been programmed in real arithmetic for evaluation on an IBM 1130 computer.

Major steps in the method are

(i) Fourier transformation of x and y; Laplace transformation of t:

$$(x, y, t) \rightarrow (k, v, s), \qquad (\quad) \rightarrow (\underset{\approx}{\quad})$$

Boundary conditions on z = 0 are then

$$\underset{\approx}{\tau}_{zz} = 0, \qquad \underset{\approx}{u}_x = \frac{4\pi a\sigma\nu}{[s^2 + k^2\sigma^2 + v^2\nu^2]^2}, \qquad \underset{\approx}{u}_y = 0;$$

(ii) Transformation of the wave equation; and use of potentials, to derive algebraic expressions for

$$\underset{\approx}{u}(k, v, z, s).$$

The double Fourier inverse transform is taken, yielding the forward Laplace transform as an explicit double integral over the whole (k,v) plane.

(iii) Propagation poles are present, due to the moving nature of the source, and the Cagniard method of Gakenheimer and Miklowitz [5] permits manipulation of the integrand for the forward Laplace transform, until it is recognizable as the required solution in the time domain. The Cagniard path turns out to involve solution of a quartic, rather than the familiar quadratic, but this presents no computational difficulty, since the approximate solution is known, and the path is found by iterative convergence.

PROPERTIES OF THE SOLUTION: WAVEFRONTS AND SINGULARITIES

Since the rupture velocities considered are slower even than the shear wave speed, the only wavefronts generated are simply those spherical wavefronts (spreading with P and S wave speeds c_d and c_s) which emanate

from the origin of rupture itself, and which carry discontinuities in the dilatational and shear wave fields. These discontinuities are found to be a step jump in acceleration, with the radiation pattern of a double couple, but modified by directional factors

$$[c_d^2 - (\sigma^2\cos^2\phi + \nu^2\sin^2\phi)\sin^2\theta]^{-2} \quad \text{for P-waves, and}$$

$$[c_s^2 - (\sigma^2\cos^2\phi + \nu^2\sin^2\phi)\sin^2\theta]^{-2} \quad \text{for S-waves.}$$ (See Figure 1, for θ,ϕ).

Note that the S-wave factor can become large near the fault plane ($\sin\theta \sim 1$) if σ and ν approach c_s.

In common with other studies in brittle fracture, our solution in general involves stress singularities at the rupture front. The singularities are integrable, and it may be shown that the τ_{zx} singularity vanishes at $\theta = 90°$, $\phi = 0$ (plane strain region) when σ is the Rayleigh wave speed, and vanishes at $\theta = 90°$, $\phi = 90°$ (anti-plane strain) when ν is the shear wave speed. Although singularities would still be present at other azimuths ϕ, it is suggested that these special values for σ and ν are most appropriate as values for growth of an elliptical crack. These values are used throughout the numerical studies which follow.

NUMERICAL EXAMPLES, FOR RELIEF OF ZX-COMPONENT OF STRESS

The solution formulae have been evaluated for a fault growing in material with c_d = 5 km./sec., c_s = 3 km./sec., and density 2.6 gm./cm^3. Two different distances are considered, and up to four different azimuths for each distance. The source dislocation is specified completely by (5) with a = 100 cm./sec (typical of values suggested by Brune [6]) and b = 0. In the present problem, the associated value of stress drop τ_{zx} found from integrating $\dot{\tau}_{zx}$ for a point very near the crack surface) is about -160 bars. All calculations are for a receiver 1 km. from the fault surface; the first distance has $\sqrt{x^2 + y^2} = 2$ km, and the second has $\sqrt{x^2 + y^2} = 10$ km. Azimuths include those of plane and anti-plane strain, and two intermediate directions ($\phi = 30°$, $\phi = 60°$).

Figure 2 shows x and y components of acceleration, at different azimuths for the nearer distance. Typical features are the relatively low accelerations associated with P-wave energy, as compared to S, and the rapid decline of acceleration after the S-arrival. These high-frequency features are present also at this distance in Figure 3, which displays the z component of acceleration and zx-stress rate. Figure 4 shows $\ddot{u}_x$ and $\dot{\tau}_{zx}$ at the further distance, about 10 km., and the response appears to have energy principally at short periods, less than about 0.5 sec.

Accelerations in Figures 2, 3, 4 typically range up to 1 g, with some values even greater. For a stress drop of around 100 bars, accelerations would be somewhat above 1/2 g.

CONCLUSIONS

A description is given of earthquake source motions which satisfy both kinematic and dynamic requirements of shear failure on a plane fault surface. For a particular geometry, a boundary value problem can be set up for the radiated elastic motion. The solution, of qualitative interest in design studies, is used to compute sample acceleration records at distance 1 km. from a rupturing fault surface.

ACKNOWLEDGMENTS

The author thanks Drs. C. H. Scholz and L. R. Sykes for their critical review of the original manuscript. This research was supported by the Advanced Research Projects Agency of the Department of Defense, and monitored by the Air Force Cambridge Research Laboratories under Contract no. F19628-71-C-0245.

REFERENCES

1. R. Burridge and L. Knopoff: Body force equivalents for seismic dislocations. Bull. Seism. Soc. Amer. 54, pp 1875-1888, 1964.

2. N. Haskell: Elastic displacements in the near-field of a propagating fault. Bull. Seism. Soc. Amer. 59, pp 865-908, 1969.

3. R. Burridge and J. R. Willis: The self-similar problem of the expanding elliptical crack in an anisotropic solid. Proc. Camb. Phil. Soc. 66, pp 443-468, 1969.

4. Paul G. Richards: The dynamic field of a growing plane elliptical shear crack. Int. J. of Solids and Structures, accepted for publication, 1973.

5. D. C. Gakenheimer and J. Miklowitz: Transient excitation of an elastic half space by a point load traveling on the surface. J. appl. Mech. 36, Trans. A.S.M.E. 91, pp 505-515, 1969.

6. J. N. Brune: Tectonic stress and the spectra of seismic shear waves from earthquakes. J. geophys. Res. 75, pp. 4997-5009, 1970.

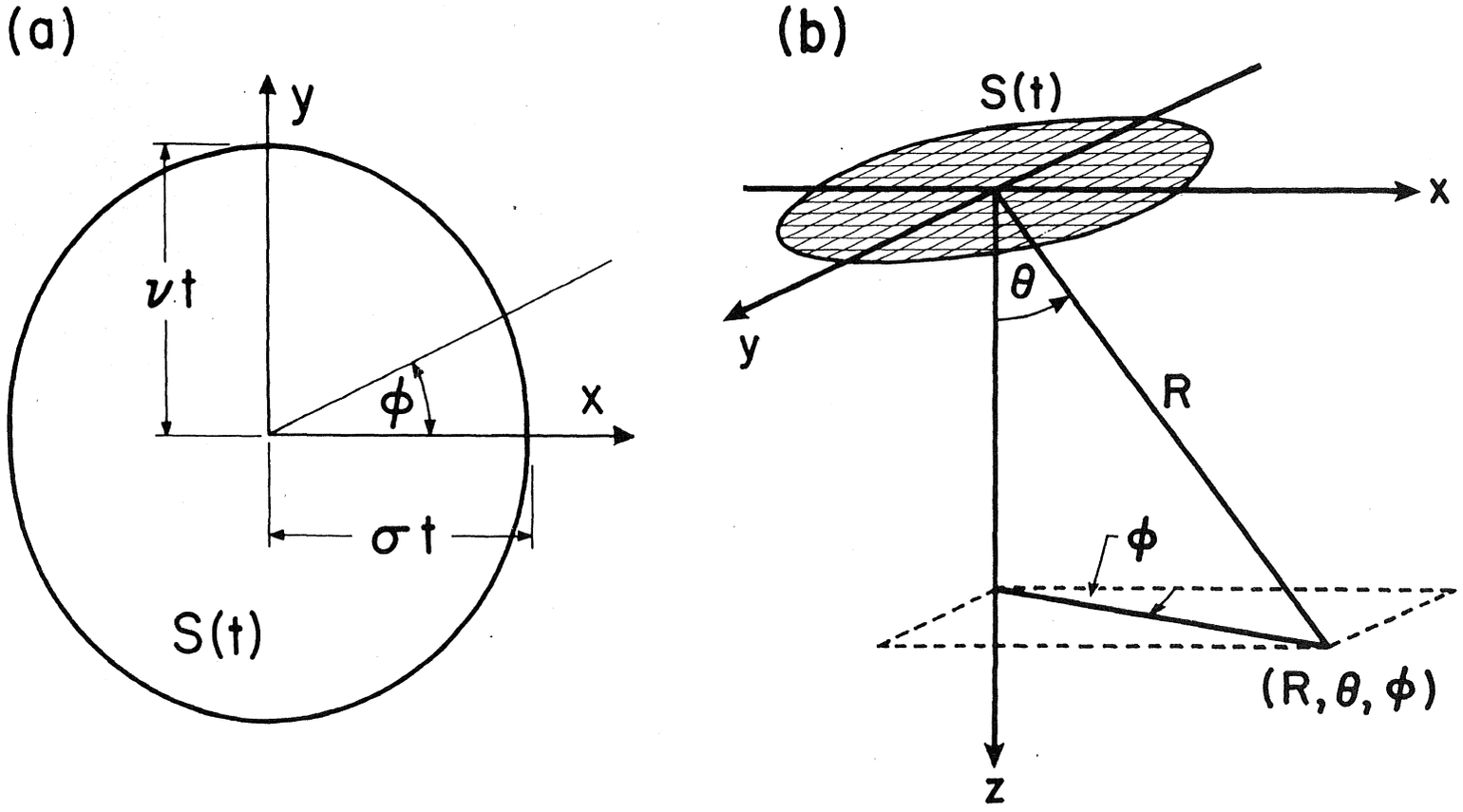

Figure 1: Parameters for a growing elliptical crack: (a) the plane $z = 0$; (b) the definition of angles (θ, ϕ).

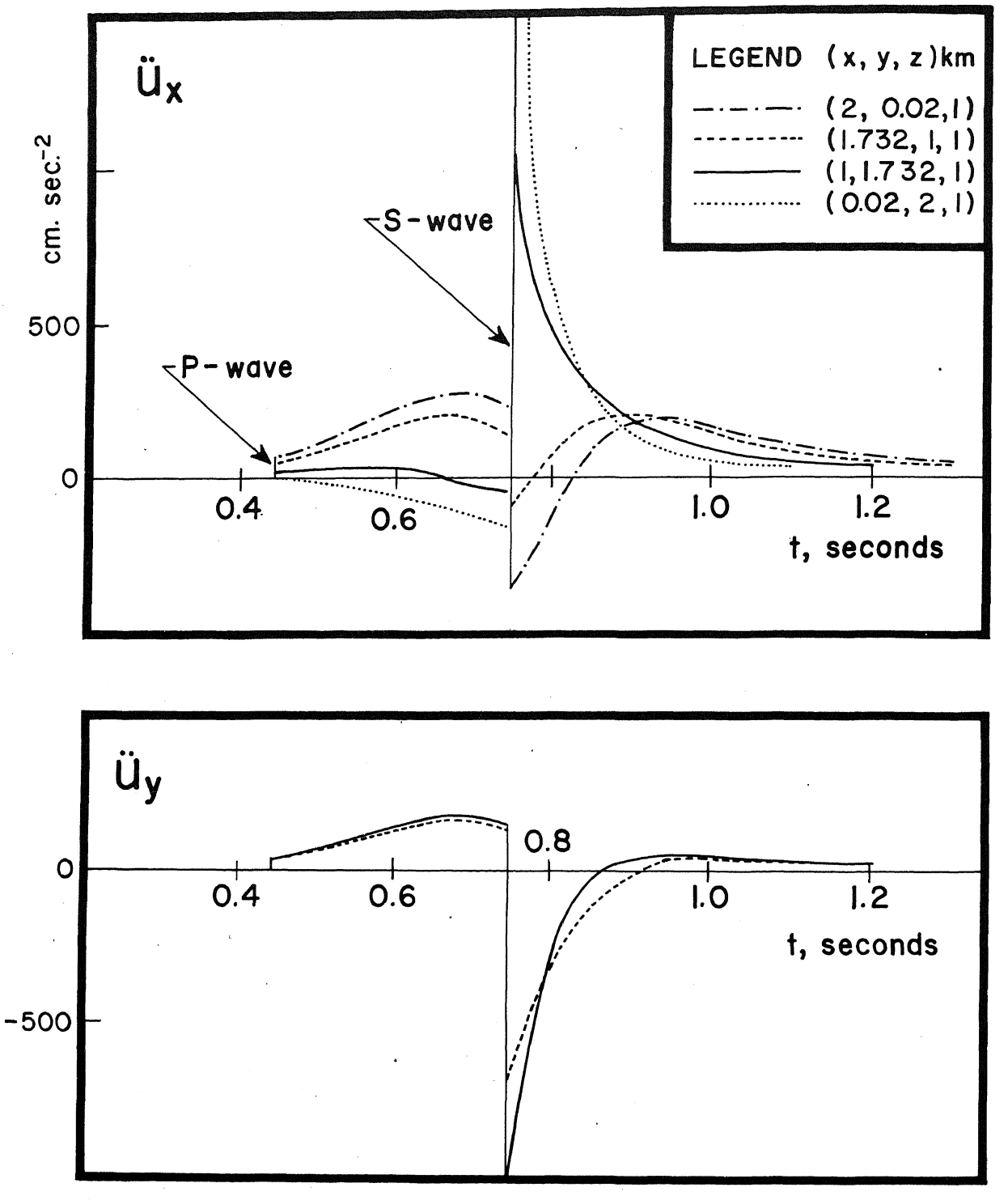

Figure 2: x and y components of acceleration, at different azimuths, for the nearer distance ~ 2 km.

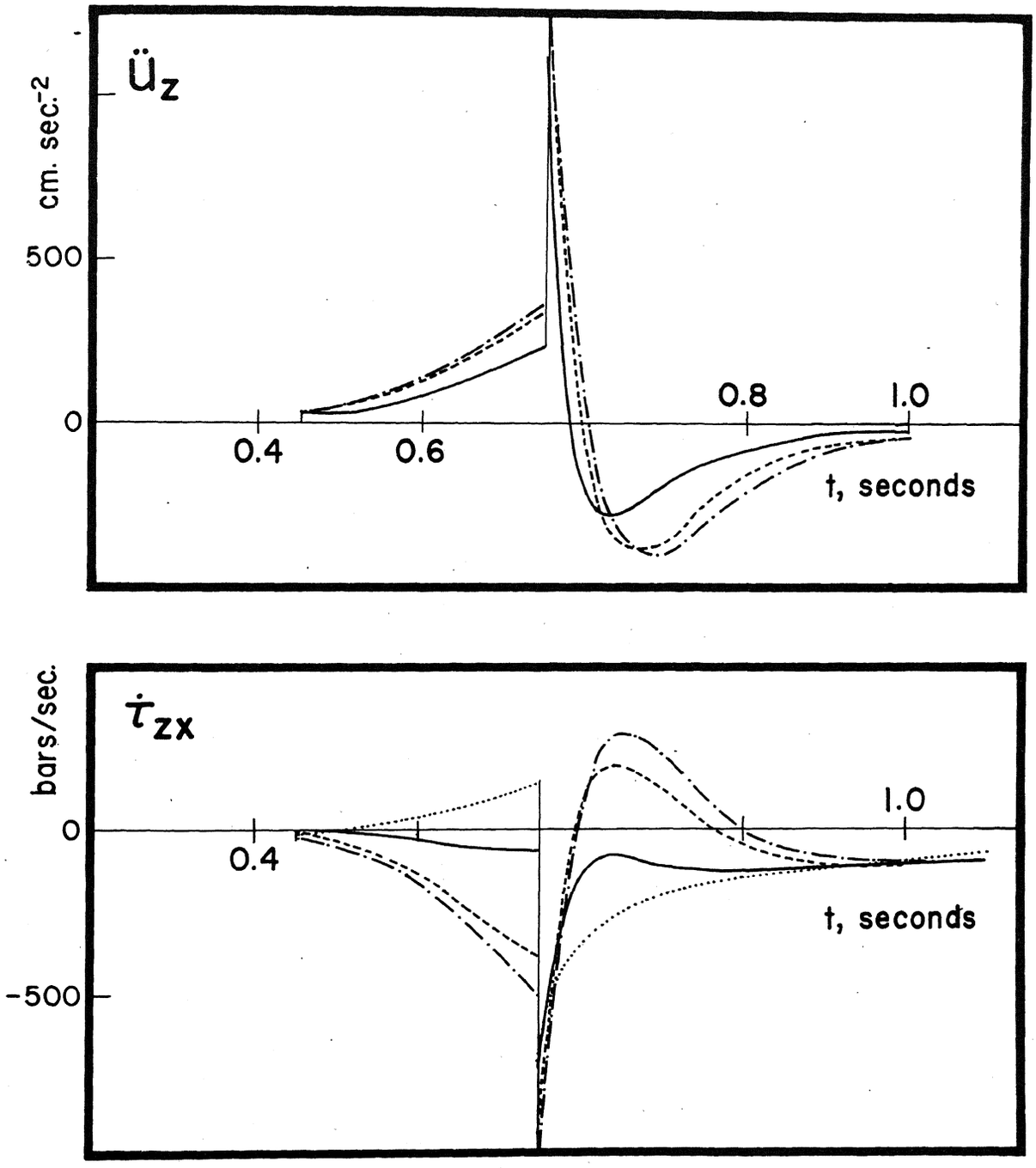

Figure 3: z component of acceleration, and zx stress rate, at different azimuths, for the nearer distance ~ 2 km. Legend as for Figure 2.

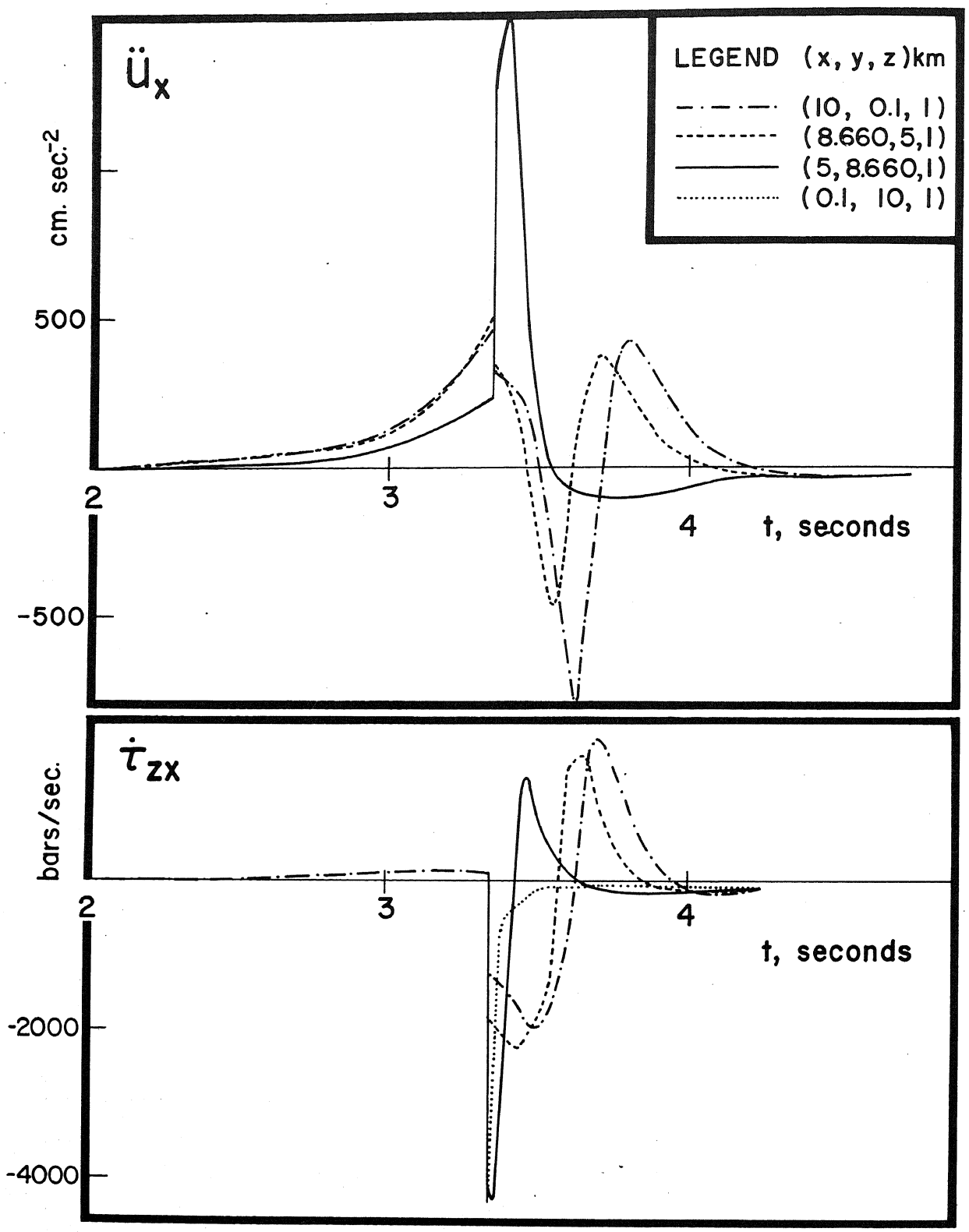

Figure 4: x component of acceleration, and zx stress rate, at different azimuths, for the further distance ~ 10 km.